Key Engineering Materials
ISSN: 1662-9795, Vol. 659, pp 446-452
doi:10.4028/www.scientific.net/KEM.659.446
© 2015 Trans Tech Publications, Switzerland

Submitted: 2015-01-02
Revised: 2015-03-20
Accepted: 2015-04-24
Online: 2015-08-18

Mechanical and Thermal properties of Silane Treated Pineapple Leaf Fiber Reinforced Polylactic Acid Composites

Supatra Pratumshat[1,2]* Phutthachat Soison[1], Sukunya Ross[1]

[1]Department of Chemistry, Faculty of Science, Naresuan University, Phitsanulok, 65000, Thailand

[2]Research Center for Academic Excellent in Petroleum, Petrochemicals and Advanced Materials, Naresuan University, Phitsanulok, 65000, Thailand

E-mail: [1*]supatraw@nu.ac.th, [1]phatthachat.soison@gmail.com, [1]sukunyaj@nu.ac.th

Keywords: Pineapple leaf fiber (PALF) composite/ Polylactic acid (PLA)/ Silane treatment/ fiber surface modification

Abstract.

In this work, the mechanical and thermal properties of pineapple leaf fiber (PALF)/poly(lactic acid) (PLA) composites were studied. PALF were pretreated with 4 %wt sodium hydroxide solution followed by various silane solutions i.e. γ-(aminopropyl) trimethoxy silane (APS), γ-methacrylate propyl trimethoxy (A174) and bis[3-(triethoxysilyl)propyl] tetrasulfide (Si69). FTIR results show a significant functional groups of C=O and C=C of methacrylic group, NH_2 group and Si-O which are the characteristic of these silane coupling agents. SEM micrographs of pretreated PALF showed a rough surface while untreated and silane treated PALF revealed less roughness. It was found that the tensile strength at break of PLA is 56 MPa and tensile strength of composites decreased when fiber content increased. The tensile modulus of silane treated PALF composites were higher than PLA, whereas their impact strength were similar to PLA. Si69 treated PALF showed lower impact strength compared to the others silanes treated fiber which indicates more phase separation between fiber and matrix. This is related to high percentage of crystallinity of composite from Si69 treated fiber. It was also found that the addition of PALF did not change the glass transition temperature and melting temperature of PLA while the percentage of crystallinity increases as the fiber content increased. In addition WAXS study of composite from Si69 treated fiber reveals sharp crystalline peaks of PLA while the others silane treatments show amorphous characteristic of PLA.

Introduction

A composite material is made by combining two or more materials often ones that have very different properties. The two materials work together to give the composite characteristic properties [1]. The best structural performance is obtained from composites that contain fibers. Since traditional fibers products do not degrade in a landfill or composting environments they pose a serious environmental problem. Therefore, natural fibers are seen as important replacement material. Also, natural fibers are renewable and relatively easily disposed of potentially recycled at the end of their lifecycle [2]. The most important of the natural fibers used in composite materials are pineapple leaf fiber, hemp, jute, kenaf, flax, cotton and sisal, due to their properties and availability [3]. The advantages of natural fibers as reinforcements are listed as: 1) low density, 2) low cost, 3) nonabrasive nature, 4) high filling level possible, 5) low energy consumption, 6) high specific properties, and 7) biodegradability [4]. In Thailand, pineapple leaf fiber (PALF) is a waste product of pineapple cultivation. Without additional cost input, PALF can be obtained for industrial purpose [5]. PALF serving as reinforcement fiber in the most of the plastic matrix has shown its significant role as it is cheap, exhibiting better properties when compare to other natural fibers. Moreover, the superior mechanical properties of PALF are associated with their high cellulose content (70-82%)[6-7]. There are a number of bio-plastics, such as Poly(lactic acid) (PLA), derived from 100% renewable sources such as corn, and the polymer is compostable [8-9]. The biodegradable aspects of such plastic are crucial to their success in replacing traditional plastics.

However, there are some drawbacks associated with a natural fiber reinforced bio-derived polymer composites, mainly their high moisture sorption and poor compatibility with hydrophobic polymer matrix leading to loss of strength in the composite [9]. To prevent this phenomenon, fiber surface have been modified in order to enhance matrix and fiber adhesion in composites [10]. In this study, the effect of silane treatment of PALF on mechanical and thermal properties of composites will be reported.

2. Materials and Methods

2.1 Materials

PLA 5060B, from NatureWorks LLC, USA was used as a matrix material. PLA pellets were dried at 80 °C for 3 h before mixing. PALF was used as a reinforcement with average length about 6 mm. Fresh chopped leaves were milled, washed with water and then dried at room temperature. After the refinement step to separate fibrous and nonfibrous part, PALF was obtained. Silane used in this work are shown in Fig. 1. They were purchased from ALDRICH.

2.2 Alkali and silane treatments

PALF was pretreated with 4 wt% solution of NaOH at room temperature for 3 h, washed with water and then dried at 80 °C for 24 h. PALF were then treated with 0.5 %v/v of silane solution in solvent mixture (6:4 v/v ethanol:water). The solution was adjusted to pH 3.5-4 and then the fibers were soaked for 2 h at room temperature. The fibers were dried at 80 °C for 24 h.

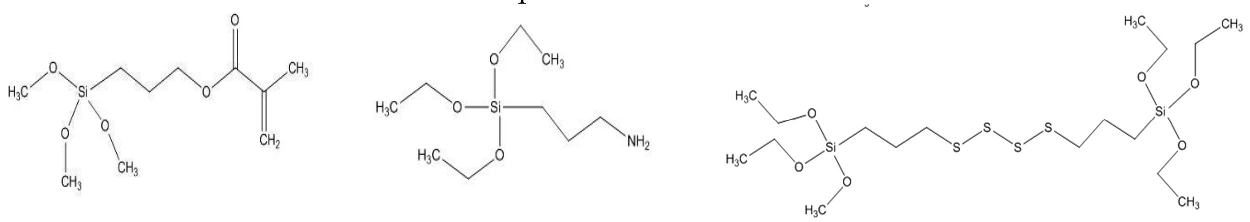

γ-methacrylate propyl trimethoxy (A174) or S1 | γ-(Aminopropyl) triethoxy silane (APS) or S2 | Bis[3-(triethoxysilyl)propyl] tetrasulfide (Si69) or S3

Fig1 Silane coupling agents used in this work

2.3 Preparation of composites

PALF and PLA were melt blended at 160 °C for 30 mins by two-rolls mill at various fiber contents (5%, 10% and 20 wt%). The samples were then compressed into 1 and 3 mm thick at 160°C.

2.4 Fourier Transform Infrared Spectroscopy (FT-IR)

PALF was mixed with KBr powder and then compressed with hydraulic press. All samples were scanned from 400 to 4000 cm^{-1} by FT-IR (Perkin-Elmer Spectrum GX).

2.5 Scanning Electron Microscope (SEM)

Fibers surface were studied using SEM, (Leo 1455VP). Samples were mounted with the carbon tapes on the aluminum stubs and then sputter coated with gold.

2.6 Differential Scanning Calorimetry Analysis

The thermal behavior of composites was studied by using DSC (Mettler Toledo, DSC1). Samples of 10-15 mg were heated from 25-200 ºC at a heating rate of 5ºC/min. Then the sample was annealed for 5 min. After that, the cooling scan was begun by cooling the sample to 25ºC at a cooling rate of 50 ºC/min. The second heating scan was performed as the same condition as the first run. The percent crystallinity was calculated by the following equation.

$$\% \text{ Crystallinity} = (\Delta H_{sample} / \Delta H_{100\%crystalline}) \times 100$$

Where ΔH_{sample} is the heat of fusion of sample (J/g). $\Delta H_{100\%crystalline}$ is the heat of fusion of pure crystalline (93 J/g for PLA, [11])

2. 7 Wide-Angle X-ray Scattering (WAXS)

WAXS experiment was examined on beam line BL1.3W: SAXS at Siam photon laboratory, Synchrotron light research institute (Public organization) (Nakhon Ratchasima, Thailand). The detector is a a Phosphore (Mar 345 Image Plate). Sample-detector distance is 140 mm and the integration time was 120 s.

2.8 Tensile testing

Tensile testing was carried out according to ASTM D 638-01. Samples were measured by tensile tester (WDW-5E) with a 1 kN-load cell. The cross-head speed was 5 mm/min and a gauge length of 50 mm. The specimens were cut into dumbbell shape as ASTM D 638 Type I. Seven samples were examined.

2.9 Impact Testing

The specimens were prepared with a 45° V-notch cutter. After notching, each specimen was placed and fixed in a position. Seven specimens were tested for each composite by impact testing machine (ITR-2000 Radmana) with a 1 kN-load cell.

3. Results and discussions

3.1 Fiber surface treatment

Fig. 2 shows the peak around 1736 and 1502 cm^{-1} for lignin and cellulose for U-PALF. For P-PALF/S2 spectra, peaks around 793 cm^{-1} and 845 cm^{-1} are attributed to the Si-C symmetric stretching. The band around 1568 cm^{-1} is the amino group of APS. The -Si-O-Si- linkage indicates the deposition of polysiloxanes on the fiber surface whereas the -Si-O-C linkage confirms the appearance of the condensation reaction between the silane coupling agent and the fibers. P-PALF/S3 spectra exhibited symmetric stretching frequencies of Si-C and Si-O-Si around 963 cm^{-1} and the asymmetric stretching of Si-O-Si and –Si-O-C identified at around 1105 cm^{-1} and 1161 cm^{-1} [5,6]. The present of the peak at 1720 cm^{-1} correspond to C=O stretching. This signal is attributed to the stretching vibrations of the carbonyl groups of S1 treated PALF [5].

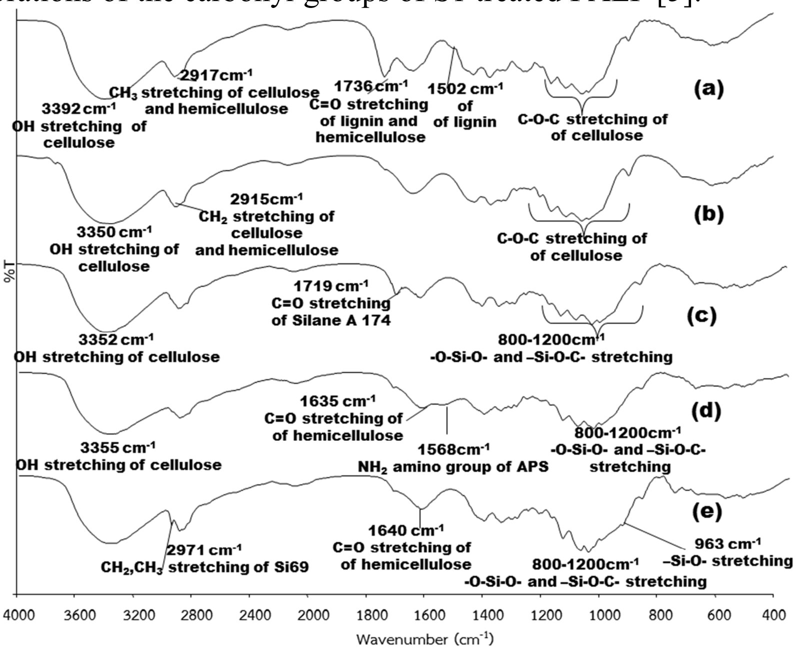

Fig. 2 FTIR spectra of (a) U-PALF, (b) P-PALF, (c) P-PALF/S1 , (d) P-PALF/S2, and (e) P-PALF/S3

*U-PALF = untreated PALF, P-PALF = pretreated PALF

3.2 Fiber morphology

Fig.3(a) shows the surface of U-PALF is covered with a layer of substances, which may include pectin, lignin, and other impurities. After NaOH treatment (Fig. 3b), lignin and pectin are removed resulting in a rougher fibers surface [1]. Fig.3 (c-e) represent the PALF after silane treatment. Silane was effectively deposited on the fiber surface and there was no dramatic change in the surface morphology as compared to alkali treated [1].

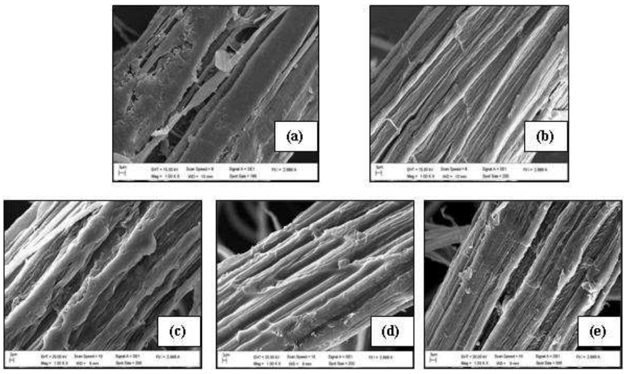

Fig. 3 SEM micrographs of (a) U-PALF, (b) P-PALF, (c) P-PALF/S1, (d) P-PALF/S2, and (e) P-PALF/S3 at magnification of 1,000x

3.4 Thermal properties

The heating thermograms of PLA show double melting peaks (not show). T_g of PLA was slightly lower than that of PALF/PLA composites. T_{cc} and T_m observed from thermograms are shown in Table 1. T_{cc} of 10% silane treated PALF composites show no significant different. Two melting peaks probably involved with the recrystallization of PLA result from variation of size crystallization of PLA. The % crystallinity of S3 composite is about 5% higher than S1 and S2 composites. This may be because of phase separation or poor adhesion between PLA and fiber. PLA chain can move easily and result in high crystalline region. S3 composite show 11% increasing in % crystallinity compared to neat PLA.

Table 1 Cold crystallization temperature, melting temperature and % crystallinity

sample	T_{cc}(°C)		T_{m1}(°C)		T_{m2}(°C)		% Crystallinity		
	T_{onset}	T_{peak}	T_{onset}	T_{peak}	T_{onset}	T_{peak}	$\%X_{c1}$	$\%X_{c2}$	$\%X_C$total
PLA	-	-	141.0	146.4	-	-	12.63	-	12.63
10% P- PALF/S1/PLA	97.2	108.5	143.5	146.9	151.1	155.8	7.43	11.34	18.77
10% P- PALF/S2/PLA	100.7	110.6	145.2	148.6	153.1	157.0	7.31	11.26	18.57
10% P- PALF/S3/PLA	98.0	110.9	144.6	148.0	152.2	156.6	8.91	15.04	23.95

$\%X_{c1}$ and $\%X_{c2}$ calculated from ΔH of T_{m1} and T_{m2}

3.5 Tensile and impact properties

Tensile strength and modulus of PLA and PLA composites are shown in Fig. 4. The U-PALF/PLA and P-PALF/PLA composites exhibit higher modulus, but lower tensile strength at break than PLA. Modulus of composites are higher, because of the introduction of fiber. NaOH treatment gave rise to modulus than PLA since it improves surface interaction between the fiber and the matrix because of mechanical interlocking brought about by an increase in surface roughness of the fiber [4]. A decreasing in strength may be due to the poor stress transfer from the matrix to the fiber as a result of weak interfacial adhesion [12]. Fig. 4(b) shows modulus increases with increasing PALF content for all silane treated composites, especially for S3 treated fiber. This is related to high percentage of crystallinity of composite from DSC result. S1 treated fiber composite show high tensile strength compare to the other silanes. This is attributed to the better interaction between the treated fiber and the matrix as a result of silane initiated crosslinking or grafting between fiber surface and matrix. Therefore, increasing adhesion between fiber and matrix results in stiff composites.

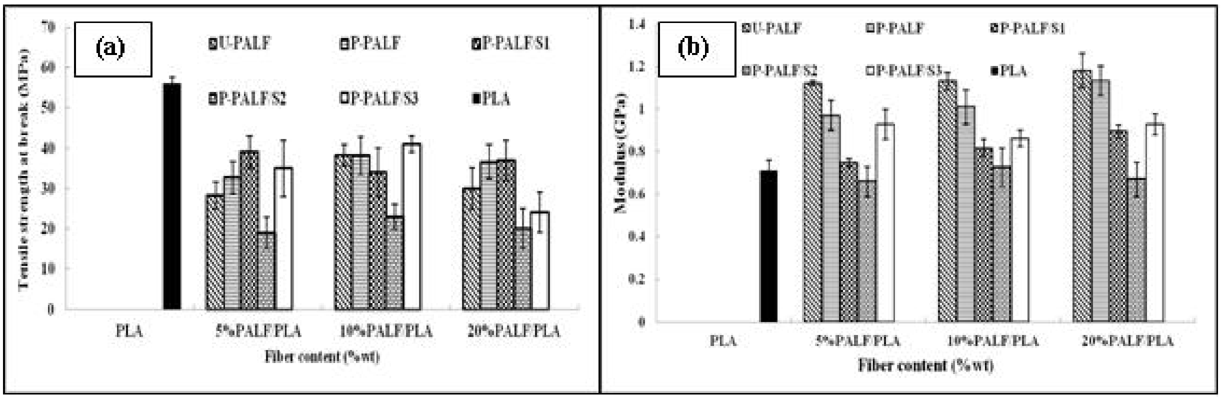

Fig. 4 Tensile properties of PLA and composites: (a) Tensile strength and (b) Modulus

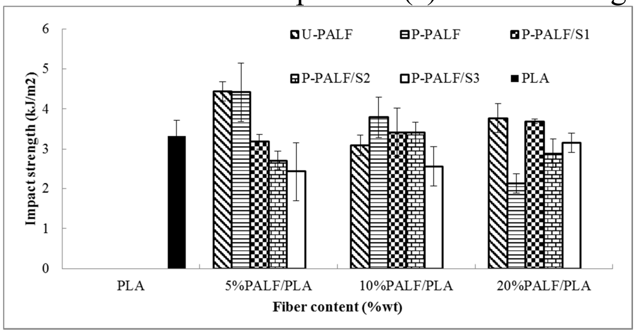

Fig. 5 Impact strength of PLA and PALF/PLA composites

Impact strength of composites (Fig.5) slightly increases with increasing amount of fiber until a weight fraction is reached at about 20%. The present of fibers decrease the energy absorbed by the specimens, addition of the fibers creates regions of stress concentrations that require less energy to initiate a crack. Impact strength of S1 composites was higher than the others.

3.6 WAXS study

WAXS technique was used to study the crystallographic structure [13]. WAXS patterns of PLA crystallized from non isothermal condition is shown in Fig.6a. It shows powder pattern and no preferred orientation. WAXS patterns of silane treated PALF composites also show powder pattern and random crystal orientation (not show in this paper). Fig.6b presents the equatorial section from WAXS pattern, silane treated fiber do not affect to the crystal orientation because of broad scattering peak. The broad peak at the scattering angle $2\theta \approx 16°$ correspond to amorphous structure of PLA. However, S3 composite show strong crystalline peaks which are similar to PLA crystallized from isothermal crystallization (see Fig 6c). This may be due to phase separation between PALF and PLA matrix, then PLA chain can move easily and crystallize into crystalline structure. Four major peaks detected are 2θ = 14.9°(010), 2θ = 16.7°(200/110), 2θ = 19.1°(203), and 2θ = 22.3°(015) [14-15]. This result was probably indicating high amount of S3 treated PALF induced crystallization of PLA. This situation is difficult to occur when low amount of fiber was added. While S1 and S2 treated fiber did not show the sharp crystalline peaks since the nature of S3 is different from S1 and S2, it is tendency to separate out from the matrix.

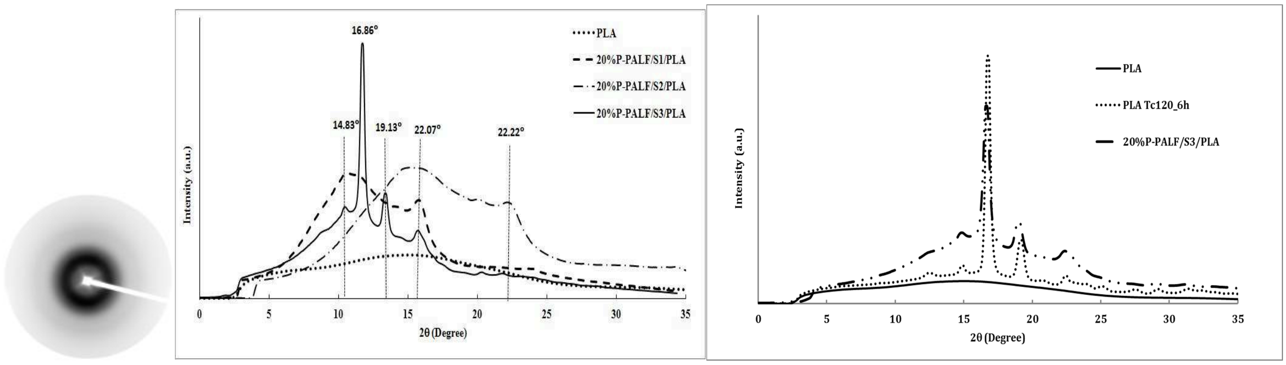

(a) (b) (c)

Fig. 6 a) WAXS pattern of PLA b) Equatorial sections of WAXS patterns of PLA, 20%P-PALF/S1/PLA, 20%P-PALF/S2/PLA, and 20%P-PALF/S3/PLA composites (c) Equatorial sections of WAXS patterns of PLA crystallized from non-isothermal, isothermal at 120 °C 6 h and 20%PALF/S3/PLA composite

Summary

The addition of fiber and fiber surface treatment have no effect on T_g, T_m and T_{cc} of PLA. % crystallinity of silane treated PALF composites is higher than that of PLA. This may be due to the effect of silane on the fiber which acting as phase separation between PLA and fiber, especially for S3. The nature of silane used in this work has effect on the compatibility between PALF and PLA matrix. Chemical treatment does not affect to the crystal orientation when samples were crystallized under non isothermal condition. However, at high content of S3 treated fiber show strong peaks of the reflection of equatorial section of WAXS pattern.

Acknowledgements

SP thanks NRCT and Faculty of Science Naresuan University for financial support. We also thank Assoc. Prof. Taweechai Amornsakchai, Mahidol University for instrument supporting for fiber preparation. WAXS experiments were measured at BL1.3W, Siam photon laboratory, Synchrotron light research institute (Public organization), Nakhon Ratchasima, Thailand.

References

[1] Faruk, O., Andrzej K. B., Fink H.P. and Sain M., Biocomposites Reinforced with Natural Fibers. Prog in Polym Sci, 37(11), (2012)1552-1596.

[2] Taj, S., Munawar Ali M., and Shafiullah K., Natural Fiber-Reinforced Polymer Composites. In Proceedings of the Pakistan Academy of Sciences**,** 44(2), (2007), 129-144.

[3] Mohanty A. K., Misra M. and Hinrichsen G., Biofibres, biodegradable polymers and biocomposites:An overview. Macromol Mat and Eng, 1,(2000), 276-277.

[4] Bledzki A. K., Reihmane S. and Gassan J., Properties and modification methods for vegetable fibers for natural fiber composites. J Appl Polym Sci, 59, (1996) 13-29.

[5] Rasal, R. M., Janorkar, A. V. and Hirt, D. E., Poly (lactic acid) modifications. Prog in Polym Sci, 35(3), (2010), 338-356.

[6] Garlotta, D., A Literature Review of Poly(Lactic Acid). J Polym and the Environ, 9, (2001), 63-84.

[7] Saha S. C., Das B. K., Ray P. K. and Pandey S. N., Pineapple Leaf Fibers and PALF-Reinforced Polymers Composites. Textile Research J, 60(12), (1990),726-731.

[8] Optical Isomer of polylactic acid. (2014, May 12). Retrieved May 12, 2014, from http://entrancechemistry.blogspot.com/2012_10_01.

[9] Lunt, J. Large-scale production, properties and commercial applications of polylactic acid polymers. Polym Degrad and Stab, 59(1),(1998), 145-152.

[10] Yasuniwa M., Iura K., and Dan Y. Melting behavior of poly(L-lactic acid): Effects of crystallization temperature and time. Polymer, 48, (2007), 5398-5407.

[11] Jong-W. R., Amar K. M., Sher P. S. and Perry K. W. N., Effect of the processing methods on the performance of polylactide films: Thermocompression versus solvent casting. J Appl Polym Sci, 101(6),(2006), 3736-3742.
[12] Hon D. N.-S., Chemical modification of lignocellulosic materials: old chemistry, new approaches, Polymer. News, 17(4), (1992), 102.
[13] Saw C. K. , X-Ray Scattering Techniques for Characterization of Nanosystems in Lifescience. Nanotechnologies for Life Sciences, (3), (2005),1-25.
[14] Michell R. M., Crystallization and Stereocomplexation Behavior of Poly(D- and L-lactide)-b-poly(N,N-dimethylamino-2-ethyl methacrylate) Block Copolymers. J Polym Sci Part B: Polym phys, 49(19), 1397-1409.
[15] Mano J. F., Wang Y., Viana J. C., Denchev Z. and Oliveira M. J., Cold crystallization of PLLA studied by simultaneous SAXS and WAXS. Macromol Mat and Eng, 289(10), (2004), 910-915.